

# On Testing of Charpy Specimens Using the One-point Bend Impact Technique

by D. Rittel, A. Pineau, J. Clisson, and L. Rota

**ABSTRACT**—This paper reports our methodology and results for the assessment of the dynamic fracture energy of notched Charpy A508 steel specimens. The fracture tests consist of one-point bend impact applied to the specimen in contact with an instrumented bar. Fracture is caused by the inertia of the unsupported specimen only. The fracture energy is determined from the incident, reflected and single wire fracture gage signals. High-speed photographic recordings show that for all the specimens investigated in the “lower shelf” temperature regime, fracture occurs relatively early and prior to “taking off” of the bar by rigid body motion. It also confirms that the fracture gage readings indeed coincide with the formation of a crack from the notch tip.

The present methodology is relatively easy to implement, and it allows the investigation of the fracture properties of materials at loading rates (and velocities) that are substantially higher than those achieved in a conventional Charpy test. Moreover, this test is attractive for modeling purposes since its boundary conditions are simple and well defined.

**KEY WORDS**—Charpy, dynamic fracture, one point bend impact, instrumented bar, high-speed photography

## Introduction

Dynamic fracture properties of many engineering materials are most generally assessed using the well-known Charpy test.<sup>1</sup> Charpy testing is the most popular dynamic characterization test in the industry.<sup>2</sup> This test, which is easily performed on a simple notched beam specimen, yields information on the global fracture energy. By global, it is meant that the various components of the impact energy are all accounted for, including strain, kinetic and fracture energies. Modeling of this experiment has been a challenge for many years, and whereas a thorough literature survey of this topic is beyond our scope, the reader may refer to recent work in order to gain insight into the problem.<sup>3–8</sup> One additional difficulty inherent to this test is that there may be a temporary loss of contact between the specimen and the tip of the impactor, thus causing the boundary conditions to vary in an uncontrolled manner.<sup>9,10</sup>

In a conventional Charpy test, the impact velocity seldom exceeds 5 m/s, thus setting a limit on the experiment. While this limit is not exceeded, it is by no means a limitation

of the concept but rather a limitation of the setup. Experimental dynamic fracture mechanics has developed considerably in the last decade and accurate methods to determine the dynamic fracture toughness of materials have been devised, all of which apply to precracked specimens. Whereas several methods (specimen, loading device and data processing) were proposed, specific advantage has been taken of the specimen inertia to perform fracture tests on unsupported specimens, under highly transient impact conditions. Such methods, called “one-point (bend) impact experiments,” have been applied to various precracked specimen geometries (beams,<sup>11,12</sup> compact compression specimens,<sup>13,14</sup> notched plates,<sup>15</sup>) for which a suitable methodology was developed to assess the dynamic initiation toughness. Typically, the specimen is either impacted directly and the crack-tip fields are monitored directly through optical techniques,<sup>16,17</sup> or the specimen is in contact with one or two instrumented bars and the boundary conditions (force/displacement) are determined from gage readings.<sup>18</sup> As an example, the dynamic fracture toughness of tungsten base heavy alloys was measured using the one point impact technique applied to small precracked beams.<sup>12</sup> Here the response of the beam to unit impulse was calculated and subsequently used to determine the critical stress intensity factor (fracture toughness) reached at fracture time, as analytical solutions were not directly applicable due to the compact geometry of the specimen.<sup>18</sup> An important result was that simple modeling techniques could be used to accurately predict the crack-tip fields (comparison between calculated and measured data), provided the linear elastic fracture framework holds.

To our knowledge, the one point bend impact technique has not been applied to testing of conventional Charpy specimens. Yet this concept can be applied to *notched* Charpy specimens to determine the fracture energy, in the spirit of the previously mentioned work. The relevant parameters are, as previously, the fracture time and applied boundary loads and displacements. However, a key difference with the previously mentioned work is that, to adhere to the philosophy of the Charpy test, the emphasis is put here on a (global) fracture energy, and not on a stress intensity factor. The present paper reports our results on the application of one point impact experiments to determine the fracture energy of steel specimens at high ( $v_{\text{imp}} \gg 5$  m/s) impact velocities.

The paper is organized as follows: in the following section, we describe the experimental framework and relevant equations needed to determine the above-mentioned parameters. Next we present and discuss the experimental results and fracture energies obtained for a specific grade of bainitic

---

D. Rittel and A. Pineau are Professors, Ecole des Mines de Paris, Centre des Matériaux P.M. Fourt, Cedex, France. J. Clisson is an Engineer and L. Rota is a (TITLE), Centre Technique de l'Armement, Cedex, France.

Original manuscript submitted: February 13, 2001.

Final manuscript received: February 4, 2002.

steel (A508) used for the fabrication of pressurized water nuclear reactors. The final section comprises a discussion on the method and the results, followed by conclusions.

## Experimental Setup and Data Processing Technique

### The Setup

The experimental setup comprises the specimen, the apparatus used to apply and measure the applied loads, the detection of the onset of fracture and the real time monitoring of the fracture process, as described next.

The fracture specimen geometry used in this study is the standard Charpy V-notch specimen (45° angle), with a length of 55 mm and a cross section of 10 mm × 10 mm. At mid-length, a 0.25 mm root radius, 2 mm deep notch is machined. A single wire fracture gage (MM-CD-02-15A) is cemented immediately ahead of the notch either on one or both sides of the specimen. The gage triggers a simple homemade clock device which delivers an electric pulse when the gage is fractured. The material selected for this study is a French steel (16MND5), of composition given in Table 1, which corresponds to A508 steel. This steel is used in the nuclear industry for pressure water vessel applications. The material was heat treated to a hardness HV (20g) = 200, with room temperature yield strength of  $\sigma_y = 500$  MPa, tensile strength  $\sigma_{uts} = 620$  MPa, and tensile elongation  $el = 10.6\%$ .

To apply and measure transient loads, an instrumented maraging steel bar (2 m long, 10 mm diameter) is used to transmit the stress wave induced by the impact of a 0.4 m long steel striker fired at velocities of the order of 25 m/s. Such a setup is simply “half” a split Hopkinson pressure bar.<sup>18</sup> The stress wave is measured on a strain gage (5 mm) cemented at 0.765 m from its free edge. The signal is recorded on a 12 bit-10 MHz digital Nicolet oscilloscope (sampling frequency 5 MHz).

The specimen is unsupported, i.e., it lays in contact with the bar, without supports to restrain the free body motion subsequent to the stress wave loading. A very thin layer of coupling grease is inserted at the specimen-bar interface to improve the impedance matching between the two. In a typical experiment, the stress wave propagates toward the specimen ( $\epsilon_{in}$ , incident pulse) and subsequently reflects partly ( $\epsilon_{ref}$ , reflected pulse) after delivering some of its initial energy to the specimen.

Direct visualization of the fracture process is achieved through high speed photography. An image converting camera (Hadland Imacon 790) is facing the specimen to take a sequence of 8 photographs, with a calibrated interframe and exposure time of 4.432  $\mu$ s and 1  $\mu$ s, respectively. The camera is initially focused on the notch, with a sufficient width of field to capture a global view of the impacted specimen and the edge of the bar. The camera is triggered by the strain pulse measured on the incident bar after insertion of a suitable delay.

The various components of the experimental setup are shown in Fig. 1. A typical experimental record thus consists of the incident and reflected pulses, the fracture gage(s) reading and (eventually) a high-speed photographic sequence. Therefore, the specimen is stress wave loaded, fractures and then leaves the bar as a result of rigid body motion. It is then “softly recovered” in a rug filled box. The exact timing of these events is determined and discussed in the results section.

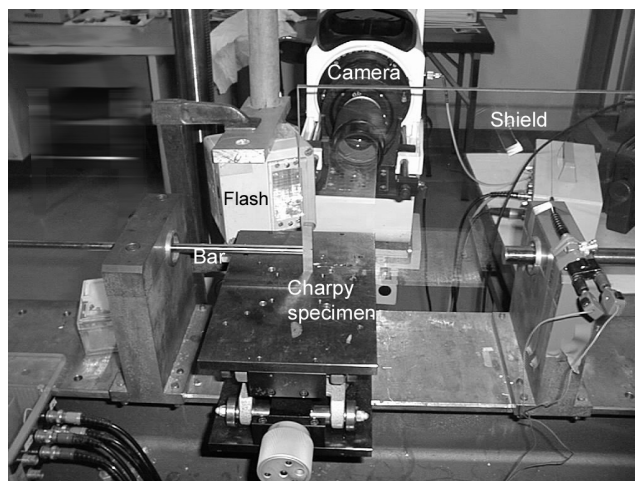


Fig. 1—Photograph showing the experimental setup. The Charpy specimen is in contact with the instrumented bar, facing the high speed camera. The single wire fracture gage is cemented on the opposite side and is thus not visible. Data is acquired on a digital oscilloscope.

### Data Reduction

The experimental signals are processed using a home made computer program, in which a correction for geometrical dispersion has been carried out, as described, e.g., in Ref. 12. The relevant equations are given below, based on the standard assumptions of one-dimensional wave propagation of elastic waves.<sup>19</sup> The load applied to the specimen is given by

$$F(t) = AE [\epsilon_{in}(t) + \epsilon_{ref}(t)], \quad (1)$$

where  $A$  and  $E$  are the bar cross section and Young's modulus, respectively. The displacement of the edge of the bar (specimen-bar interface) is given by

$$u(t) = c_0 \int_0^t [\epsilon_{in}(\alpha) - \epsilon_{ref}(\alpha)] d\alpha, \quad (2)$$

where  $c_0$  is the longitudinal wave velocity.

Finally, the impact energy delivered to the specimen is written as

$$W = Ac_0E \int_0^{t_f} [\epsilon(\alpha)_{in}^2 - \epsilon(\alpha)_{ref}^2] d\alpha, \quad (3)$$

where  $t_f$  is the fracture time.

Some remarks can be made on these equations. First, it should be noted that the load (eq (1)) can only be applied to the specimen as long as the latter is in contact with the bar. Once it leaves the bar, a free edge condition prevails, which is characterized by a load free state. Consequently, independently of the duration of the incident pulse, the actual load is ultimately determined by the specimen and the “take-off” conditions.

By contrast, the displacement of the edge of the bar (eq (2)) will be a boundary condition for the specimen as long as the latter is in contact with the bar. Past this time, however, the

TABLE 1—NOMINAL SPECIMEN COMPOSITION IN W/O (FE BAL.)

C	S	P	Si	Mn	Ni	Cr	Mo	Cu	Co	V
0.16	0.004	0.008	0.22	1.33	0.76	0.22	0.51	0.07	0.0017	<0.01

bar will continue to advance, and a nonzero signal will still be measured.

Finally, eq (3) is all that is needed to actually assess the energy imparted to the specimen (while eqs (1) and (2) are useful to obtain eq (3)), provided the actual fracture time  $t_f$  is measured.

Visual assessment is useful in two important respects: the first is the determination of the specimen “take-off” time vs. fracture time. The second information is the correlation between the fracture gage readings and visual detection of the crack, and eventually its velocity. It is well known that accurate determination of the onset of fracture is a bottleneck in all dynamic fracture experiments. This information is necessary to set the upper integration limit for eq (3). These issues are discussed in the next section.

## Results

### Preliminary Considerations

In order to fracture a specimen successfully, the specimen has to be sufficiently “brittle” to fracture rather than deform upon impact. Preliminary experiments showed that this situation is attained when the specimens are tested at a relatively low temperature. For the steel investigated in this study, this corresponds to the “lower shelf” regime. To cool the specimen it was dunked in liquid nitrogen, let cool down and then extracted. The time elapsed until the experiment was measured. In a separate experiment, a specimen instrumented with two thermocouples (one attached to the surface, the second at mid-thickness along the notch) was used to establish a cooling and a heating curve from liquid nitrogen. As expected for a steel specimen with these dimensions,<sup>20</sup> almost no difference was found between the core and surface temperatures. The thermal calibration was used in the subsequent experiments to determine the specimen’s temperature at impact.

### Specimen “take-off” Time

The first point to be determined is that of the time at which the specimen actually leaves the bar. To that purpose, several experiments were carried out at room temperature, where fracture does not take place. Figure 2 shows the typical response of an uncracked specimen to the impact. The recording shows that the specimen is increasingly flying away from the bar as time elapses. The first evidence of a faint gap between the specimen and the bar visible at earlier times than 82.5  $\mu$ s (time 2 on Fig. 3), with the origin of time being measured when the stress wave first reaches the specimen. This time is determined from the wave velocity and the specimen to strain gage distance. The gap is fully visible on the next frame, taken at 87  $\mu$ s. Figure 3 shows the superposed raw incident and reflected signals. It can be noted that the reflected level reaches that of the incident after a time lapse of 80  $\mu$ s (time 1), thus indicating that the force has decreased to zero (eq (1)). The small difference in the estimation of the “take-off” time results from the use of two different techniques.

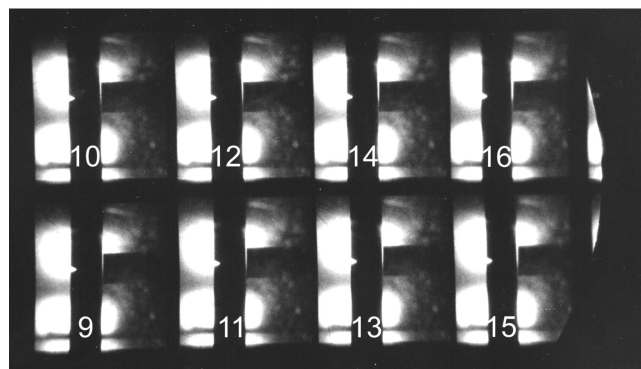
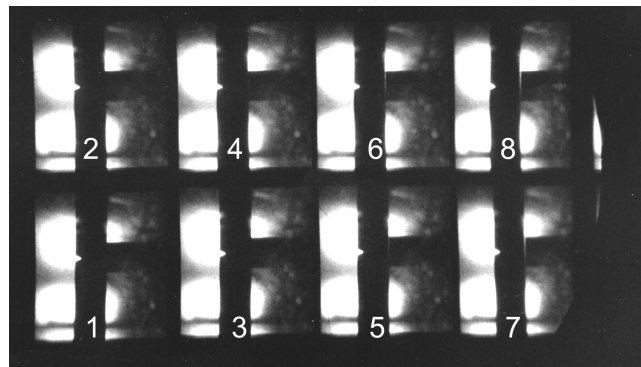


Fig. 2—High speed photograph of a Charpy specimen subjected to impact loading. Time origin is taken when the stress wave reaches the specimen. This photographs comprises two distinct experiments (frames 1-8 and 9-16), to illustrate the overall response of the specimen. Frame 1 is taken at  $t = 69.25 \mu$ s and frame 9 is taken at  $t = 119.25 \mu$ s. Interframe and exposure times for each picture are 4.432  $\mu$ s, and 1  $\mu$ s respectively. Note the faint gap between the specimen and the bar on frame 4 at  $t = 82.5 \mu$ s, indicating specimen “take off”. In this experiment, the specimen did not fracture.

Visual identification of the gap has inherent limitations, and accurate estimation of the beginning of the incident/reflected signals has an absolute error of typically 1  $\mu$ s. Consequently, this experiment reveals that the specimen remains in contact with the bar during a typical duration of 80  $\mu$ s, with very good agreement between gage readings and photographic evidence. Incidentally, it can be noted that this time is much larger than the characteristic time associated with a roundtrip of the waves in a 10 mm thick specimen (about 4  $\mu$ s). This can be explained by the fact that the specimen is not a cylinder as in conventional split Hopkinson pressure bar tests, in which the wave transit is considered as one-dimensional.

### Typical Results

A typical plot (specimen CHH33) of the signals, processed as a force-time diagram, is shown in Fig. 4. In this figure, fracture is recorded 32.3  $\mu$ s after the stress wave reaches the specimen. It can be noted that fracture is detected beyond the

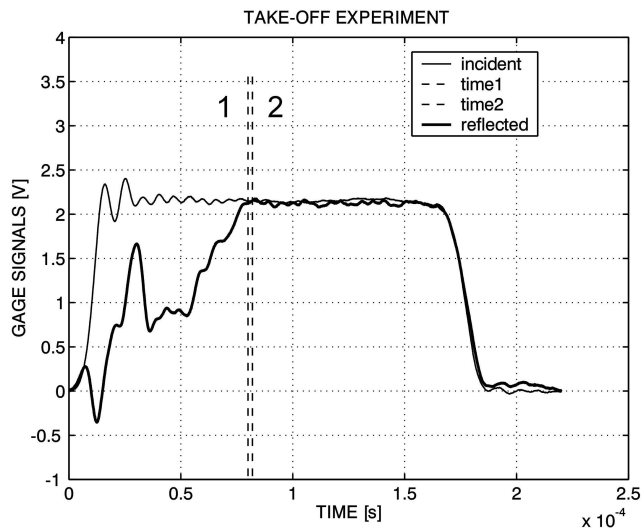


Fig. 3—Superposed (inverted) incident and reflected signals corresponding to a typical experiment during which fracture does not occur. The signals have been corrected for geometrical dispersion. At time 1 = 80  $\mu$ s the signals reach the same level, indicating that the applied load has dropped to zero as a result of a traction free surface condition. Time 2 = 82.5  $\mu$ s is the “take-off” time estimated from Fig. 2.

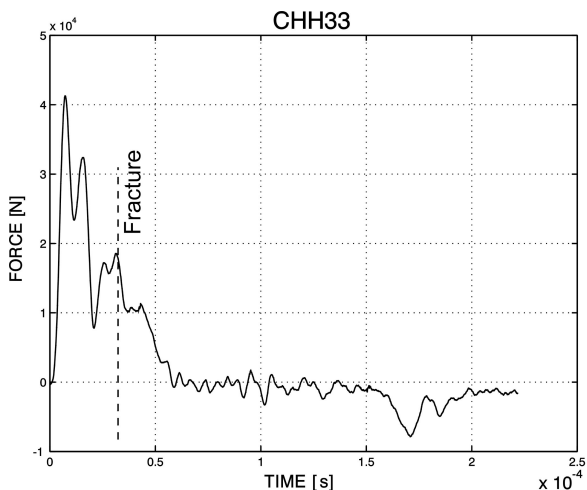


Fig. 4—Specimen CHH33. Plot of the applied load vs. time. The dashed line indicates fracture of the specimen (fracture gage). Note that fracture occurs beyond the maximal load. The force drops to zero at about 60  $\mu$ s, indicating completion of the fracture process.

maximal value of the force, as this is typically the case in dynamic fracture. This figure indicates that the load drops back to zero at about 60  $\mu$ s. This time is shorter than the previous “take-off” time of 80  $\mu$ s. It can reasonably be assumed that this difference lies in the very fact that, in the former case, the specimen did not fracture whereas in the present case, it broke in two halves. The kinetics of flight of the specimen is obviously different in each case.

The high speed picture corresponding to this experiment is shown in Fig. 5. From this figure, with a 4.432  $\mu$ s interframe time, it is noted that the fracture time indicated by the fracture gage is situated between the 4th (taken at 29.5  $\mu$ s) and the 5th frame (taken at 34.0  $\mu$ s), closer to the 5th frame. As such

a recording is characteristic of the fracture experiments, it should also be noted that the specimen fractures while in contact with the bar. It is also concluded that, in this range of temperatures where the fracture is “brittle,” the fracture gages provide a reliable indication of the onset of crack propagation (fracture).

### Fracture Results

A total number of 8 Charpy specimens were tested at various temperatures, as shown in Table 2. In the selected range of temperatures corresponding to the “lower shelf” (up to 137K), all the specimens fractured in two halves. In all the cases, the impact velocity was of the order of 25 m/s, which is about 5 times that of a typical Charpy experiment. None of the recorded fracture times exceeded 43  $\mu$ s, that is all specimens fractured prior to leaving the bar. The fracture energy, determined in these experiments lies in the range of 7-11 J. These values should be compared with fracture energies determined in a conventional Charpy test carried out at the same temperature. This comparison will be developed in a subsequent paper, whereas the emphasis is presently put on the experimental approach.

### Discussion

This paper reports new results on the inertial fracture of Charpy steel specimens. Several interesting issues have been investigated in this work. Firstly, the experiments show that notched Charpy specimens can actually be fractured inertially, provided their temperature is sufficiently low. While the test is restricted to the “lower shelf” regime, it nevertheless provides useful information on the fracture energy and failure mechanisms at high(er) impact velocities, when compared with conventional Charpy tests. This information is all the more important since there is little information available on the variations of fracture energy with loading rate in the “lower shelf regime.” More generally, this method applies to materials that are sufficiently “brittle” to fracture under given impact conditions. It is therefore not restricted to the “lower shelf” regime as it applies to nonferrous materials as well. Moreover, one-point impact experiments are characterized by simple boundary conditions, a fact that makes these tests attractive for modeling purposes.

A critical issue is that of the detection and timing of fracture. Fracture time is the upper limit for the calculation of the fracture energy, as shown in eq (3). Therefore, monitoring of the fracture process should be as accurate as possible. In previous work on precracked heavy alloy specimens, it was found that the single wire fracture gages provided an accurate indication of the onset of crack propagation, when compared with crack-tip strain gages signals.<sup>12</sup> The correspondence between fracture gage readings and high-speed photography of the crack development supports this conclusion. However, one must keep in mind that all the methods mentioned so far (gages, photography) monitor the free surface of the specimen. At present, actual monitoring of the crack-front through the specimen thickness is still lacking for these kinds of experiments.<sup>17</sup> This may not be critical as long as three-dimensional effects (tunneling) are negligible. Unfortunately, this is not always the case, as may sometimes be noted from the front shape of arrested cracks that are subsequently opened. Our low temperature experiments always caused the specimen to fracture in two pieces without

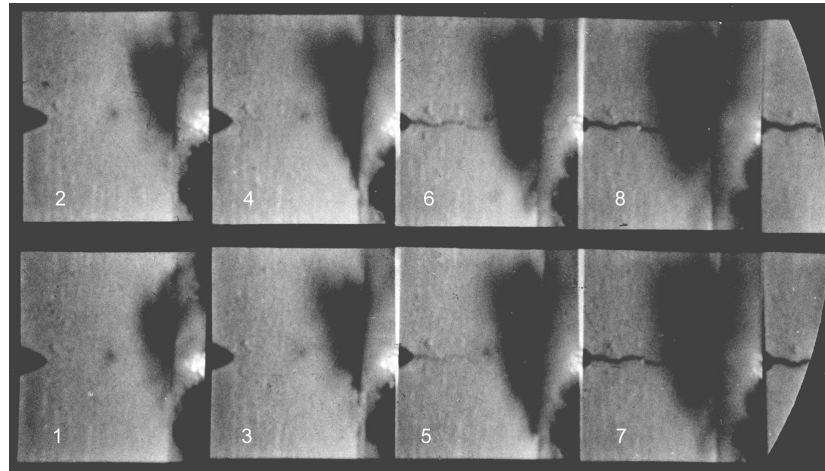


Fig. 5—Specimen CHH33. High speed photograph with indicated exposure times. A crack is clearly observed to form between the 4th and 5th frame. Fracture was detected by the fracture gage at 32.3  $\mu$ s, close to the 5th frame (34  $\mu$ s).

TABLE 2—EXPERIMENTAL RESULTS AND TEST TEMPERATURES

Specimen	Temperature [K]	Time [ $\times 10^{-6}$ s]	Fracture Energy [J]
CHH28	116	35.05	8.90
CHH29	125	29.25	9.00
CHE14	125	39.70-42.20	10.33-11.03
CHH30	137	29.50	8.50
CHH31	137	33.10	11.24
CHE13	137	28.10-29.40	7.80-8.05
CHE15	139	28.60-35.60	7.60-9.30
CHH33	149	32.30	11.10

Paired values correspond to the use of 2 fracture gages, one on each side of the specimen. Subsequent testing with the high-speed camera was carried out with one gage only.

noticeable shear lips. As a first approximation, one will suppose that tunneling effects were not predominant. Otherwise, the measured fracture energy should be considered as an upper bound value since fracture is always detected in its latest phase on the sides of the specimen.

Another important result is the accurate determination of the time at which the specimen loses contact with the incident bar. The high-speed photographs definitely show that, on the average, fracture precedes specimen “take off” by some 30 to 40  $\mu$ s. While the “take off” time cannot be correlated to the specimen dimensions in a straightforward manner, it can nevertheless be identified as the instant at which the incident and reflected signals reach a similar level, or in other words the time at which the applied load drops to zero. This instant could clearly be observed in the experiments. It is worth noting that in the case of smaller precracked specimens (23 mm long, 10 mm wide and 8 mm high), the force dropped to zero at around 40  $\mu$ s, and here too, all the specimens fractured prior to “take off.”<sup>12</sup> In this case, reducing the length to about half its original value while leaving the width and height relatively unchanged shortens the “take off” time in the same ratio. These results provide useful information that can be related to the analytical predictions of the “test duration.”<sup>11</sup>

One may wonder about the validity of such experiments for the potential case where the specimen would fracture after “taking off” the bar. The impact energy divides continuously into strain, fracture, and kinetic energy. It has been reported that the kinetic energy of the broken fragments of Charpy

steel specimens tested in the lower shelf, is of the order of 2 J.<sup>21</sup> On the other hand, as long as the specimen is loaded by the bar, it deforms and thus possesses a large strain energy component.<sup>11</sup> The exact distribution and evolution of these energies is beyond the scope of the present paper, as in any standard Charpy test during which a *global* impact energy is measured. Consequently, the fact that a specimen may “take off” prior to fracturing should not be considered as a limiting factor for the present test, as long as a global energy is to be measured.

## Conclusions

The one-point bend impact method has been successfully applied to the investigation of the dynamic fracture energy of A508 steel Charpy specimens. The following conclusions can be drawn:

- One-point impact can be successfully applied to high velocity Charpy testing of sufficiently “brittle” materials.
- The specimen’s “take off” time is identified as the time at which the load drops to zero.
- The fracture time, as determined from single wire fracture gages, provides a reliable estimate of the onset of crack propagation. Fracture energy can be determined subsequently.

- In the present experiments, the specimens fractured prior to “taking off” of the bar.

### Acknowledgments

Professor T. Thomas (CTA) is acknowledged for his promotion and participation to this cooperative research.

### References

1. Charpy, M.G., “Note sur l’essai des métaux à la flexion par choc de barreaux entaillés,” *Soc. Ing. Français*, 848–877 (1901).
2. Siewert, T.A., Manahan, M.P., McCowan, C.N., Holt, J.M., Marsh, F.J., and Ruth, E.A., “The History and Importance of Impact Testing,” in *Pendulum Impact Testing: A Century of Progress*, STP1380, 1–16, ASTM, West Conshohocken, PA (1999).
3. Norris, Jr., D.M., “Computer Simulation of the Charpy V-notch Toughness Test,” *Eng. Frac. Mechanics*, **11**, 261–274 (1979).
4. Tvergaard, V. and Needleman, A., “Effect of Material Rate Sensitivity on Failure Modes in the Charpy V-notch Test,” *J. Mech. Phys. Solids*, **34** (3), 213–241 (1986).
5. Böhme, W., Sun, D.Z., Schmitt, W., and Höning, A., “Application of Micromechanical Material Models to the Evaluation of Charpy Tests,” in *Advances in Fracture/Damage Models for the Analysis of Engineering Problems*, AMD, **137**, 203–216, ASME, New York, NY (1992).
6. Mathur, K.K., Needleman, A., and Tvergaard, V., “3D Analysis of Failure Modes in the Charpy Impact Test,” *Modeling Simul. Mater. Sci. Eng.*, **2**, 617–635 (1994).
7. Rossoll, A., “Détermination de la ténacité d’un acier faiblement allié partir de l’essai Charpy instrumenté,” Ph.D. thesis, Ecole Centrale des Arts et Manufactures, Châtenay-Malabry, France (1998).
8. Tahar, M., “Applications de l’approche locale de la rupture fragile à l’acier 16MND5,” Ph.D. thesis, Ecole Des Mines de Paris, Paris, France (1998).
9. Kalthoff, J.F., Winkler, S., and Beinert J., “The Influence of Dynamic Effects in Impact Testing,” *Int. J. Fract.*, **13**, 528–531 (1977).
10. Kalthoff, J.F., Winkler, S., Böhme, W., Shockey, D.A., in *Proc. International Conference on the Dynamical Properties and Fracture Dynamics of Engineering Materials*, Brno, Czechoslovakia (1983).
11. Giovanola, J.H., “Investigation and Application of the One-point Bend Impact Test,” *Fracture Mechanics: Seventeenth Volume*, ASTM-STP 905, J. H. Underwood and R. Chait et al., eds., 307–328 (1986).
12. Weisbrod, G. and Rittel, D., “A Method for Dynamic Fracture Toughness Determination Using Short Beams,” *Int. J. Fract.*, **104** (1), 89–103 (2000).
13. Bui, H.D., Maigre, H. and Rittel, D., “A New Approach to the Experimental Determination of the Dynamic Stress Intensity Factor,” *Int. J. Solids Structures*, **29** (23), 2881–2895 (1992).
14. Rittel, D., Maigre, H., and Bui, H.D. A New Method for Dynamic Fracture Toughness Testing, *Scripta Metallurgica et Materialia*, **26**, 1593–1598 (1992).
15. Rittel, D. and Levin, R., “Mode-mixity and Dynamic Failure Mode Transitions in Polycarbonate,” *Mechanics of Materials*, **30** (3), 197–216 (1998).
16. Beinert, J. and Kalthoff, J.F., “Experimental Determination of Dynamic Stress Intensity Factors by Shadow Patterns,” In *Mechanics of Fracture 7*, G.C. Sih, ed., 281–330 (1981).
17. Aoki, S. and Kimura, T., “Finite Element Study of the Optical Method of Caustic for Measuring Impact Fracture Toughness,” *J. Mech. Phys. Solids*, **41** (3), 413–425 (1993).
18. Rittel, D. and Maigre, H., “An Investigation of Dynamic Crack Initiation in PMMA,” *Mechanics of Materials*, **28**, 229–239 (1996).
19. Kolsky, H., *Stress Waves in Solids*, Dover Publications Inc., New York, NY (1963).
20. Rabin, Y. and Rittel, D., “Infrared Temperature Sensing of Mechanically Loaded Specimens: Thermal Analysis,” *EXPERIMENTAL MECHANICS*, **40** (2), 197–202 (2000).
21. Kalthoff, J.F., Waldherr, U., and Takahashi, S., “Fracture Energy of Ceramics Measured at Different Loading Rates in Instrumented Impact Tests,” *J. de Physique IV, Colloque C3*, **1**, 693–699.